View metadata, citation and similar papers at core.ac.uk
brought to you by CORE
provided by Yamaguchi University Navigator for Open access Collection and Archives

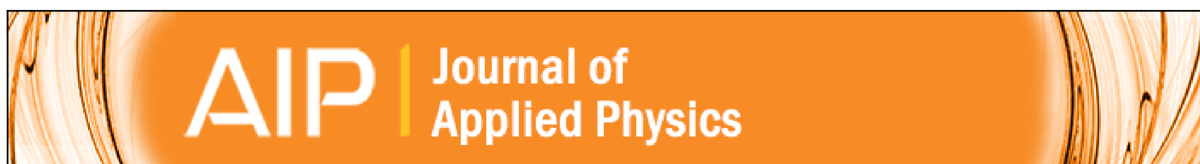

Si concentration dependence of structural inhomogeneities in Si-doped Al x Ga1− x N/Al y Ga1− y N multiple quantum well structures (x=0.6) and its relationship with internal quantum efficiency

Satoshi Kurai, Koji Anai, Hideto Miyake, Kazumasa Hiramatsu, and Yoichi Yamada

Citation: Journal of Applied Physics **116**, 235703 (2014); doi: 10.1063/1.4904847
View online: http://dx.doi.org/10.1063/1.4904847
View Table of Contents: http://scitation.aip.org/content/aip/journal/jap/116/23?ver=pdfcov
Published by the AIP Publishing

Articles you may be interested in
Reduction in the concentration of cation vacancies by proper Si-doping in the well layers of high AlN mole fraction Al x Ga1– x N multiple quantum wells grown by metalorganic vapor phase epitaxy
Appl. Phys. Lett. **107**, 121602 (2015); 10.1063/1.4931754

Spatial clustering of defect luminescence centers in Si-doped low resistivity Al0.82Ga0.18N
Appl. Phys. Lett. **107**, 072103 (2015); 10.1063/1.4928667

Excitonic localization in AlN-rich AlxGa1−xN/AlyGa1−yN multi-quantum-well grain boundaries
Appl. Phys. Lett. **105**, 122111 (2014); 10.1063/1.4896681

Inhomogeneous distribution of defect-related emission in Si-doped AlGaN epitaxial layers with different Al content and Si concentration
J. Appl. Phys. **115**, 053509 (2014); 10.1063/1.4864020

Investigation of Mg doping in high-Al content p -type Al x Ga 1 − x N (0.3 x 0.5)
Appl. Phys. Lett. **86**, 082107 (2005); 10.1063/1.1867565

The new SR865 2 MHz Lock-In Amplifier ... $7950

Chart recording

FFT displays

Trend analysis

Features
· Intuitive front-panel operation
· Touchscreen data display
· Save data & screen shots to USB flash drive
· Embedded web server and iOS app
· Synch multiple SR865s via 10 MHz timebase I/O
· View results on a TV or monitor (HDMI output)

Specs
· 1 mHz to 2 MHz
· 2.5 nV/√Hz input noise
· 1 µs to 30 ks time constants
· 1.25 MHz data streaming rate
· Sine out with DC offset
· GPIB, RS-232, Ethernet & USB

Stanford Research Systems
www.thinkSRS.com · Tel: (408)744-9040

Reuse of AIP Publishing content is subject to the terms at: https://publishing.aip.org/authors/rights-and-permissions. Download to IP: 133.62.137.102 On: Wed, 16 Mar 2016 07:53:26

JOURNAL OF APPLIED PHYSICS **116**, 235703 (2014)

Si concentration dependence of structural inhomogeneities in Si-doped $Al_xGa_{1-x}N/Al_yGa_{1-y}N$ multiple quantum well structures ($x = 0.6$) and its relationship with internal quantum efficiency

Satoshi Kurai,[1,a)] Koji Anai,[1] Hideto Miyake,[2] Kazumasa Hiramatsu,[2] and Yoichi Yamada[1]
[1]*Department of Material Science and Engineering, Yamaguchi University, 2-16-1 Tokiwadai, Ube, Yamaguchi 755-8611, Japan*
[2]*Department of Electrical and Electronic Engineering, Mie University, 1577 Kurimamachiya, Tsu, Mie 514-8507, Japan*

(Received 6 October 2014; accepted 7 December 2014; published online 19 December 2014)

We investigated the distribution of luminescence in Si-doped $Al_xGa_{1-x}N/Al_yGa_{1-y}N$ multiple quantum well (MQW) structures ($x = 0.6$) with different Si concentrations by cathodoluminescence (CL) mapping combined with scanning electron microscopy. The effects of surface morphology, dark spot density, and full width at half-maximum of spot CL spectra on internal quantum efficiency (IQE) were determined. A flat surface morphology and uniform CL map were observed for Si-doped AlGaN MQWs, in contrast to undoped AlGaN MQW and Si-doped AlGaN with relatively low Al content. The dark spot density in the Si-doped AlGaN MQWs increased exponentially as the Si concentration increased and did not explain the Si concentration dependence of IQE. In contrast, there was a clear correlation between the dark spot density and IQE of the AlGaN MQWs at a constant Si concentration. The emission energy distribution arising from the inhomogeneity of the relative Al content and the well layer thickness was estimated by monochromatic CL measurements, although there was almost no difference in the distribution for different Si concentrations. Therefore, the previously reported dependence of the defect complexes on Si concentration is reflected in the IQE of Si-doped AlGaN MQWs. Defect complexes composed of cation vacancies and impurities rather than dislocations and interfacial quality are the major contributor to the IQE of the Si-doped AlGaN MQWs with different Si concentrations. © *2014 AIP Publishing LLC*.
[http://dx.doi.org/10.1063/1.4904847]

I. INTRODUCTION

$Al_xGa_{1-x}N$ ternary alloys are attractive candidates for ultraviolet (UV) light emitters and detectors. UV emitters that produce light at the most effective germicidal wavelength of 265 nm, where UV absorption by DNA is highest, could be used for sterilization. Excitons in wide-gap semiconductors have a large exciton binding energy, which is comparable to room temperature (RT) thermal energy. Recently, biexciton (excitonic molecules) luminescence of the $Al_{0.61}Ga_{0.39}N$ ternary alloy was observed at RT and its binding energy was measured as 56 ± 4.4 meV.[1] Thus, $Al_xGa_{1-x}N$ ternary alloys with a relative Al content (x) of around 0.60, which corresponds to their spectral wavelength of around 265 nm, are important for both device applications and optical physics. The internal quantum efficiency (IQE) of Al-rich AlGaN ternary alloys is drastically reduced at shorter wavelengths.[2–4] The IQE of AlGaN ternary alloy also depends strongly on dislocation density.[5,6] Recently, the efficiency of deep UV AlGaN based light-emitting diodes (LEDs) has been increased by the improvement of growth techniques and the development of high-quality substrates.[2] However, the emission efficiency of LEDs is still low because the large activation energy of the acceptors results in high resistivity of p-type Al-rich AlGaN. In an alternative approach, electron-beam-pumped UV light sources have been demonstrated that use hundreds of Al-rich AlGaN multiple quantum wells (MQWs) as targets and do not require p-type AlGaN.[7,8]

Si doping of an $Al_xGa_{1-x}N$ epitaxial layer changes its structural, electrical, and optical properties, including strain state,[9,10] surface morphology,[10–13] dislocation inclination,[2,13] electrical conduction,[14] luminescence intensity,[15] point defects,[16] and optical polarization.[17] The relationship between these changes is complicated, and the effects of Si doping in III-nitrides are not fully understood. It is important to investigate these effects to fabricate high-efficiency devices. We previously reported the effects of Si doping on the surface morphology and microscopic distribution of cathodoluminescence (CL) in AlGaN ternary alloys with a high relative Al content.[10] Hexagonal hillocks formed as the Si concentration increased, and local donor-acceptor pair emission around the hillocks was observed. This type of inhomogeneity in AlGaN ternary alloys degrades device performance and must be measured carefully, particularly in thin film quantum devices. The IQE of Si-doped AlGaN MQW structures has been examined at different Si concentrations.[18] The IQE of AlGaN MQWs initially increased and then decreased with increasing Si concentration in the well layers. This was explained by the variation in the interface quality and the concentration of point defects.

[a)]Email: kurai@yamaguchi-u.ac.jp

 © 2014 AIP Publishing LLC

Reuse of AIP Publishing content is subject to the terms at: https://publishing.aip.org/authors/rights-and-permissions. Download to IP: 133.62.137.102 On: Wed, 16 Mar 2016 07:53:26

TABLE I. Summary of sample characteristics. All samples were $Al_xGa_{1-x}N/Al_yGa_{1-y}N$ MQW structures deposited on a c-plane sapphire (0001) substrate with AlN (0.8 μm), AlGaN intermediate layers (0.2 μm), and a 0.4-μm-thick Si-doped AlGaN layer.

Sample set	1. Different Si concentration in well layers	2. Different barrier layer thickness
Relative Al content *x*	0.60	0.60
Relative Al content *y*	0.74	0.70
Well layer thickness (nm)	1.5	1.5
Barrier layer thickness (nm)	4.7	3.0, 7.0, 11.0, 15.0
Number of quantum wells	100	137, 75, 50, 38
Si concentration in the well layer (cm^{-3})	3.8×10^{17}, 7.6×10^{17}, 1.1×10^{18}	3.8×10^{17}
Si concentration in the barrier layer (cm^{-3})	3.8×10^{17}	3.8×10^{17}

In this work, we studied the Si concentration dependence of the structural and optical inhomogeneities in Si-doped $Al_xGa_{1-x}N/Al_yGa_{1-y}N$ MQW structures ($x = 0.6$) by CL combined with scanning electron microscopy (SEM), and then the results were compared with the IQE results. We discuss the relationship between the surfaces, density of defects, the alloy and thickness inhomogeneity, and the IQE in Si-doped AlGaN MQW structures.

II. EXPERIMENTAL

The $Al_xGa_{1-x}N/Al_yGa_{1-y}N$ MQW structures used in the present work were grown by low-pressure metal-organic vapor phase epitaxy on c-plane sapphire substrates, following the deposition of a 0.8-μm-thick AlN buffer layer, a 0.2-μm-thick Al-rich AlGaN intermediate layer, and a 0.4-μm-thick Si-doped AlGaN layer.[8] Two sample sets of $Al_xGa_{1-x}N/Al_yGa_{1-y}N$ MQW structures were prepared. (1) MQW structures consisting of 100 1.5-nm-thick $Al_{0.60}Ga_{0.40}N$ well layers separated by 4.7-nm-thick $Al_{0.74}Ga_{0.26}N$ barrier layers with different Si concentrations in the well layers and a constant Si concentration of $3.8 \times 10^{17}\,cm^{-3}$ in the barrier layers. The Si concentrations in the well layers were 3.8×10^{17}, 7.6×10^{17}, and $1.1 \times 10^{18}\,cm^{-3}$. (2) MQW structures consisting of 137, 75, 50, and 38 1.5-nm-thick $Al_{0.60}Ga_{0.40}N$ well layers separated by 3.0, 7.0, 11.0, and 15.0-nm-thick $Al_{0.70}Ga_{0.30}N$ barrier layers, respectively, with a constant Si concentration of $3.8 \times 10^{17}\,cm^{-3}$ in the well and barrier layers. Si concentrations were estimated from secondary ion mass spectrometry (SIMS) measurements of AlGaN thin films. The detection limit of the SIMS measurement for Si concentration is less than $1 \times 10^{16}\,cm^{-3}$. The sample structures of the two sample sets are summarized in Table I.

CL mapping measurements combined with SEM were performed with an Oxford Mono-CL2 CL detector attached to a Hitachi S-4300SE microscope at an acceleration voltage of 2.5 kV and a sample current of around 150 pA. The SEM and panchromatic CL measurements were carried out at RT for comparison with the IQE results. The CL spectroscopic measurements were carried out at 80 K. The spectral resolution of the CL spectrum was ± 0.18 nm, which corresponds to ± 3.6 meV around 250 nm. IQEs were evaluated by temperature- and excitation-power-density-dependent photoluminescence (PL) spectroscopy. Details of the IQE measurement method are described in Refs. 18 and 19.

III. RESULTS AND DISCUSSION

Figure 1 shows surface SEM images and panchromatic CL images of undoped and Si-doped AlGaN MQW structures at RT. The Si concentration of the Si-doped AlGaN MQW was $3.7 \times 10^{17}\,cm^{-3}$. Hexagonal hillocks were observed on the surface SEM image of the undoped AlGaN MQWs, although no specific features were observed on the surface of the Si-doped AlGaN MQW. In the panchromatic

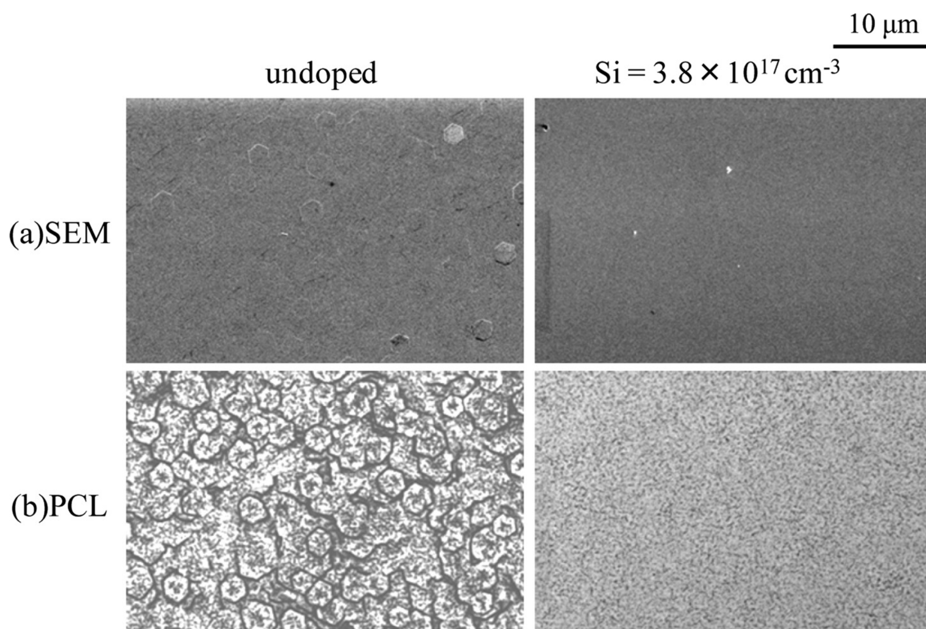

FIG. 1. (a) Surface SEM images and (b) panchromatic CL images of undoped and Si-doped $Al_{0.60}Ga_{0.40}N/Al_{0.74}Ga_{0.26}N$ MQW structures taken at RT.

Reuse of AIP Publishing content is subject to the terms at: https://publishing.aip.org/authors/rights-and-permissions. Download to IP: 133.62.137.102 On: Wed, 16 Mar 2016 07:53:26

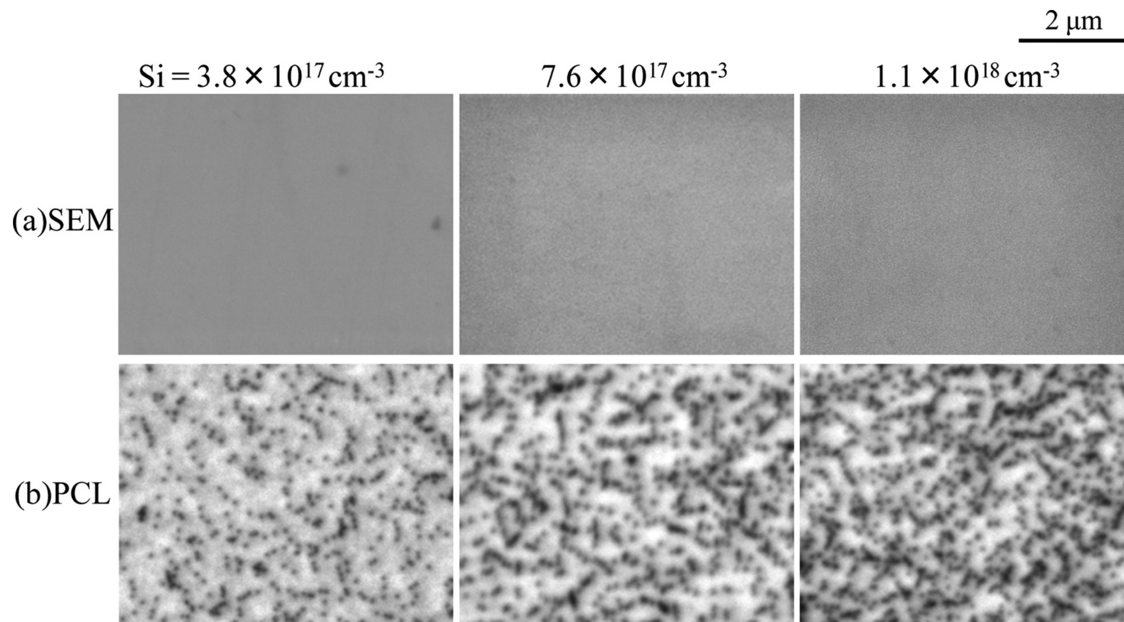

FIG. 2. High magnification (a) surface SEM images and (b) panchromatic CL images of Si-doped $Al_{0.60}Ga_{0.40}N/Al_{0.74}Ga_{0.26}N$ MQW structures with different Si concentrations in the well layers taken at RT.

CL image, the hexagonal contrast corresponding to the surface morphology and numerous dark spots were observed in undoped AlGaN MQW structures. In contrast, there were uniform dark spots and no hexagonal contrast in Si-doped AlGaN MQW structures.

These results are consistent with the previous study of strain states in Si-doped AlGaN epitaxial layers, in which compressive strain was increased and lattice relaxation was suppressed by light Si doping below a Si concentration of about $3.7 \times 10^{17}\,cm^{-3}$.[10] The suppression of lattice relaxation by light Si doping prevents the introduction of dislocations into AlGaN MQWs.

Flat surfaces and uniform panchromatic CL images were also observed for Si-doped AlGaN MQWs with higher Si concentrations in the well layers at RT (Fig. 2). In our previous studies of AlGaN epitaxial layers, hexagonal hillock density strongly depended on Si concentration[11] and relative Al content,[20] and increased with increasing Si concentration and with decreasing relative Al content. Hillocks were still observed in the AlGaN epitaxial layer with a relative Al content of 0.60 and Si concentration of $3.8 \times 10^{17}\,cm^{-3}$, which are almost same as in the well layers of Si-doped AlGaN MQWs. We were concerned whether hillocks would form on these AlGaN MQWs. However, we obtained flat surfaces at Si concentrations of up to $1.1 \times 10^{18}\,cm^{-3}$, probably because the barrier layers had a higher relative Al content, which accounts for 75% of total MQW thickness, and arises from the relatively low Si concentration. Thus, we can now allay concerns about large structural inhomogeneities in $Al_{0.60}Ga_{0.40}N/Al_{0.74}Ga_{0.26}N$ MQWs.

The dark spots in the AlGaN MQWs represent threading dislocations that act as non-radiative recombination centers, and are related to the IQE.[5,6] Discrete dark spots are visible in the panchromatic CL images in Fig. 2(b). The number of dark spots increased with the Si concentration. Figure 3 shows the dark spot densities estimated from Fig. 2(b) plotted as a function of Si concentration. The dark spot densities of the order of $10^9\,cm^{-2}$ in AlGaN MQWs were consistent with the estimated threading dislocation density from ω-scan X-ray rocking curves.[18] Therefore, dark spot density observed in panchromatic CL images corresponds to threading dislocation density. Figure 3 shows an exponential increase in dark spot density with Si concentration. This trend is also explained by the increase in the lattice relaxation in Si-doped AlGaN epitaxial layers with increasing Si concentration at concentrations greater than $3.7 \times 10^{17}\,cm^{-3}$.[10]

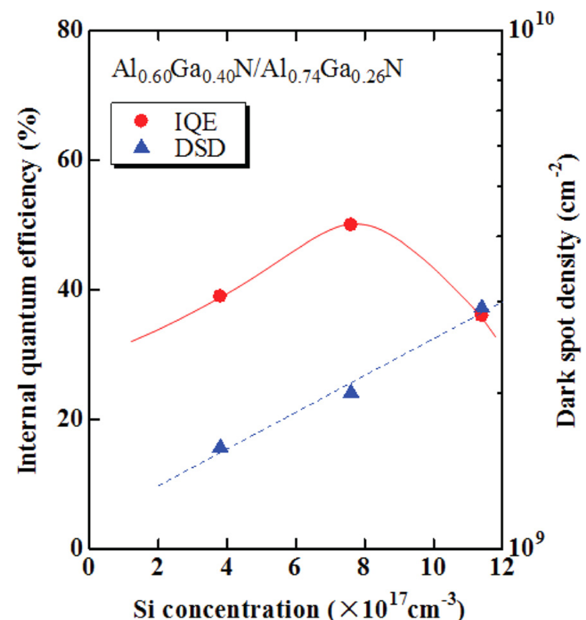

FIG. 3. Si concentration dependence of IQEs estimated by Murotani *et al.*[18] (filled circles) and dark spot density (filled triangles) of Si-doped $Al_{0.60}Ga_{0.40}N/Al_{0.74}Ga_{0.26}N$ MQW structures with different Si concentrations in the well layers.

Reuse of AIP Publishing content is subject to the terms at: https://publishing.aip.org/authors/rights-and-permissions. Download to IP: 133.62.137.102 On: Wed, 16 Mar 2016 07:53:26

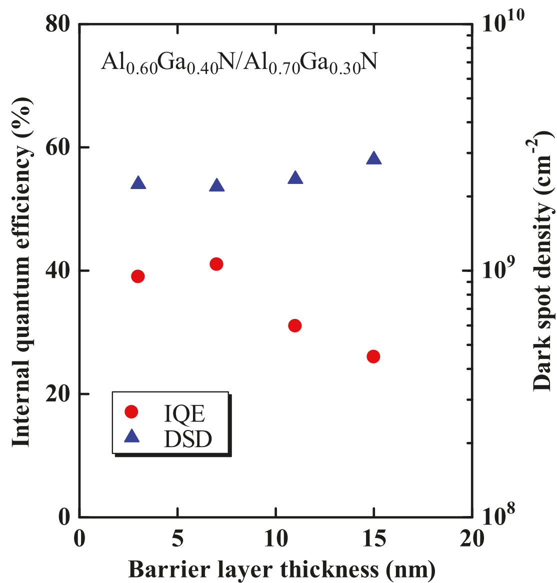

FIG. 4. Barrier layer thickness dependence of IQE (filled circles) and dark spot density (filled triangles) of Si-doped $Al_{0.60}Ga_{0.40}N/Al_{0.70}Ga_{0.30}N$ MQW structures with a constant Si concentration in the well layers and different barrier layer thicknesses.

The IQEs estimated by Murotani *et al.* for the same AlGaN MQWs at RT are also shown in Fig. 3.[18] The Si concentration dependence of the IQE, which initially increases and then decreases, is different from that of the dark spot density. To discuss the effects of Si doping on IQE and dark spot density, SEM and panchromatic CL images of AlGaN MQWs with different barrier thicknesses, which have a different dislocation density and the same Si concentration, were obtained at 80 K. Smooth surface and uniform panchromatic CL images were obtained for the AlGaN MQWs with different barrier thicknesses. Figure 4 shows the dark spot density and IQE of AlGaN MQWs as a function of the barrier layer thickness. The dark spot density increases with the barrier layer thickness. The dislocation density was probably altered by the difference in the strain state of AlGaN MQWs with different barrier layer thicknesses. In contrast to the Si concentration dependence, reducing the dark spot density in AlGaN MQW with a constant Si concentration increases the IQE. This indicates that the dark spots, which act as nonradiative recombination centers, still affect the IQE of AlGaN MQWs at a constant Si concentration. However, there must be an additional factor that reduces the IQE of AlGaN MQWs with different Si concentrations. As mentioned above, Murotani *et al.* explained the dependence of IQE on Si concentration by variations in the interface quality and the concentration of point defects.

To confirm the energetic uniformity of the MQW structure, CL spectra and monochromatic CL images were taken at 80 K for AlGaN MQWs with different Si concentrations in the well layers. Because the wide area ($26 \times 19\ \mu m^2$) integrated scanning CL spectra of AlGaN MQWs showed a single emission peak around the band edge, monochromatic CL images were taken at the lower-energy side at half-maximum, and at the higher-energy side at half-maximum of the near band edge emission. Figure 5 shows monochromatic CL images of AlGaN MQWs with different Si concentrations in the well layer taken at these energies. The observed distribution in the emission energy was a few micrometers in size in AlGaN MQWs, and the regions emitting at the lower-energy side and the higher-energy side of peak emission energy were complementary. The spot CL spectra obtained from limited spot areas were measured at the positions emitting at the lower-energy side (L1 and L2 in Fig. 5) and the higher-energy side of peak emission energy (H1 and H2 in Fig. 5). The spot size was estimated to be around 200 nm from the acceleration voltage of 2.5 kV. Figures 6(a) and 6(b) show the peak energy and full width at half-maximum (FWHM) of the spot CL spectra as functions of Si concentration, respectively. Those of the scanning CL spectra are also shown for comparison.

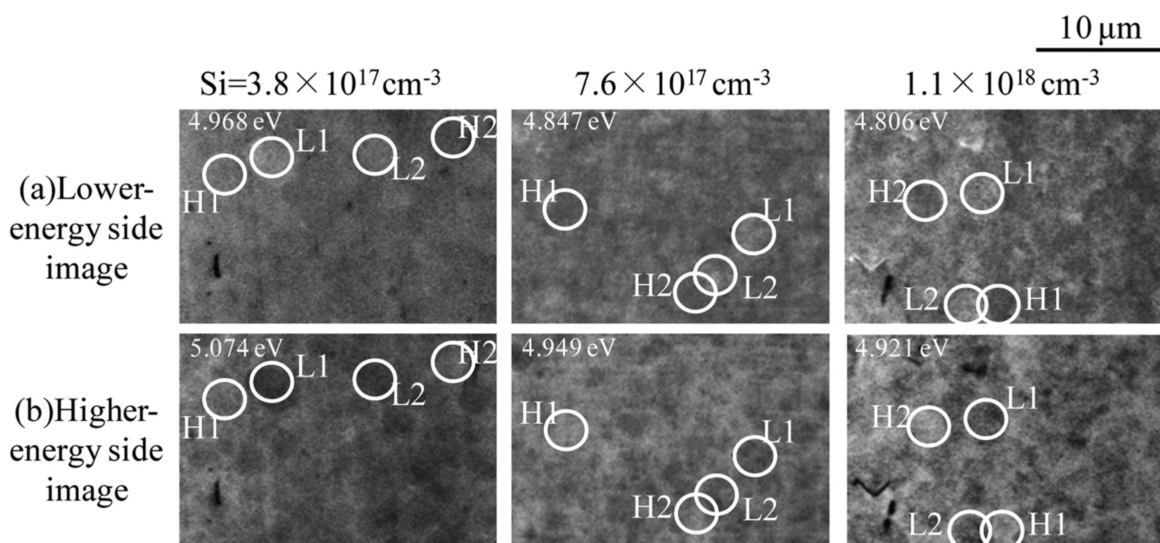

FIG. 5. Monochromatic CL images taken at 80 K for the $Al_{0.60}Ga_{0.40}N/Al_{0.74}Ga_{0.26}N$ MQW with different Si concentrations in the well layer. Images taken at (a) the lower-energy side at half-maximum and (b) the higher-energy side at half-maximum of the near band edge emission. The detection energy is also shown in the upper left of each image.

Reuse of AIP Publishing content is subject to the terms at: https://publishing.aip.org/authors/rights-and-permissions. Download to IP: 133.62.137.102 On: Wed, 16 Mar 2016 07:53:26

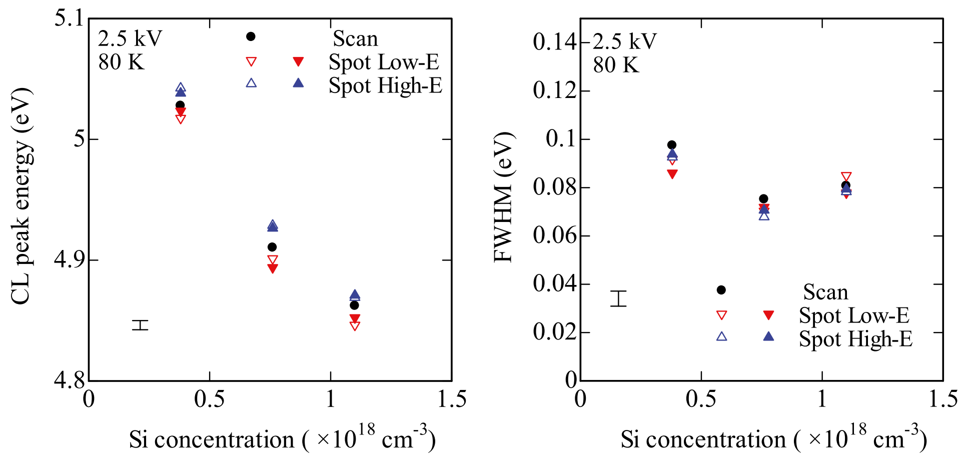

FIG. 6. CL peak energies and FWHMs of spot CL spectra taken at 80 K as a function of Si concentration in the well layers. Spot CL spectra were measured at the positions emitting at the lower-energy side (the centers of the white circles labeled L1 and L2 in Fig. 5) and the higher-energy side (the centers of the white circles labeled H1 and H2 in Fig. 5) of the peak emission energy. The spot size was estimated to be around 200 nm from the acceleration voltage of 2.5 kV. FWHMs of scanning CL spectra are shown for comparison.

In Fig. 6(a), the CL peak emission energies of the Si-doped AlGaN MQWs with different Si concentrations in the well layers are different. According to Murotani *et al.*, the PL peak energy did not change with increasing excitation power density in Si-doped MQWs, indicating that the effect of any internal electric field is negligible.[18] The shift in the CL peak energy arises from small differences in Al content and in in-plane compressive strain, which should relax in Si-doped AlGaN with increasing Si concentrations greater than $3.7 \times 10^{17}\,\mathrm{cm}^{-3}$.[10] Because the effect of the internal electric field is expected to be negligible in the Si-doped AlGaN MQWs, the effect of the change in electron-hole overlapping on the IQE should be negligible.

The difference in peak emission energy between the lower- and the higher-energy region of AlGaN MQWs with a Si concentration of $3.7 \times 10^{17}\,\mathrm{cm}^{-3}$ was about 0.03 eV. This corresponds to a variation in well thickness of less than one monolayer, calculated for a simple one-dimensional well with a finite barrier, or to the compositional fluctuation of well layers of less than 1% at a band gap energy of around 5 eV. This was observed for increasing Si concentration up to a concentration of $1.1 \times 10^{18}\,\mathrm{cm}^{-3}$ and no significant difference was observed in the monochromatic CL images. In Fig. 6(b), the FWHM of AlGaN MQWs with a Si concentration of $7.6 \times 10^{17}\,\mathrm{cm}^{-3}$ was slightly narrower, although this was not a significant difference. The FWHMs of the spot CL spectra were compared with those of the scanning CL spectra. Because the reduction ratio of the FWHMs of the spot CL spectra to those of the scanning CL spectra was the same regardless of the Si concentration, the uniformity of the emission energy within the spot size, which was estimated from the acceleration voltage as about 200 nm, did not vary substantially with the Si concentration. These results indicate that the fluctuations in the thickness and alloy composition of the AlGaN MQWs were well controlled, and the energy fluctuations in the AlGaN MQWs were not affected substantially by changes in Si concentration.

The variation of the IQE with Si concentration in the well layers was explained by the variation of interface quality and the concentration of point defects.[18] However, the changes in energy fluctuation with the Si concentration were very small in the AlGaN MQWs, and it is difficult to explain the change in the IQE by the interface quality and composition fluctuation. Thus, the variation of the defect complex concentration with Si concentration reported by Uedono *et al.*[16] explains the change in the IQE of AlGaN MQWs with Si concentration in the well layers. The defect complexes composed of cation vacancies and impurities may contribute directly to the IQE of AlGaN MQWs. In summary, the change in defect complex concentration and dislocation density in AlGaN MQWs affects the IQE, and the contribution of defect complex concentration to the change in IQE resulting from Si doping is dominant.

IV. SUMMARY

We investigated the distribution of luminescence in Si-doped AlGaN MQW structures ($x = 0.6$) with different Si concentrations by CL mapping and SEM. We compared the surface morphology, the dark spot densities, and the FWHM of spot CL spectra with the IQE. Flat surface morphology and uniform CL map was observed for Si-doped AlGaN MQWs, in contrast to undoped AlGaN MQW and Si-doped AlGaN with relatively low Al content. This is because of the relatively low Si concentration and high Al content of the samples. In addition, the maximum IQE of the Si-doped AlGaN MQWs was obtained within the Si concentration of the samples evaluated in the experiment. Thus, the Si doping of the AlGaN MQWs has little impact on the evolution of the surface hillocks and interface roughening in relation to its use for high-efficiency light sources for sterilization. The dark spot density in the Si-doped AlGaN MQWs increased exponentially with the Si concentration and could not explain the Si concentration dependence of IQE. In contrast, a clear correlation was observed between the dark spot density and IQE of the AlGaN MQWs at a constant Si concentration. The emission energy distribution arising from the inhomogeneity of the relative Al content and the well layer thickness was estimated by monochromatic CL measurements; however, the distribution was not affected by the Si concentration. Therefore, the variation of the defect complex concentration with Si concentration reported by Uedono *et al.*[16] is mainly reflected in the IQE of Si-doped AlGaN MQWs. Defect complexes composed of cation vacancies and impurities, rather than dislocations and interfacial quality, are the major contributors to the IQE of the Si-doped AlGaN MQWs with different Si concentrations.

Reuse of AIP Publishing content is subject to the terms at: https://publishing.aip.org/authors/rights-and-permissions. Download to IP: 133.62.137.102 On: Wed, 16 Mar 2016 07:53:26

ACKNOWLEDGMENTS

This work was supported by JSPS KAKENHI Grant No. 25420288.

[1]R. Kittaka, H. Muto, H. Murotani, Y. Yamada, H. Miyake, and K. Hiramatsu, Appl. Phys. Lett. **98**, 081907 (2011).
[2]H. Hirayama, N. Maeda, S. Fujikawa, S. Toyoda, and N. Kamata, Jpn. J. Appl. Phys., Part 1 **53**, 100209 (2014).
[3]A. Bhattacharyya, T. D. Moustakas, L. Zhou, D. J. Smith, and W. Hug, Appl. Phys. Lett. **94**, 181907 (2009).
[4]R. G. Banal, M. Funato, and Y. Kawakami, Appl. Phys. Lett. **99**, 011902 (2011).
[5]K. Ban, J. Yamamoto, K. Takeda, K. Ide, M. Iwaya, T. Takeuchi, S. Kamiyama, I. Akasaki, and H. Amano, Appl. Phys. Express **4**, 052101 (2011).
[6]M. Shatalov, W. Sun, A. Lunev, X. Hu, A. Dobrinsky, Y. Bilenko, J. Yang, M. Shur, R. Gaska, C. Garrett, and M. Wraback, Appl. Phys. Express **5**, 082101 (2012).
[7]T. Oto, R. G. Banal, K. Kataoka, M. Funato, and Y. Kawakami, Nature Photon. **4**, 767 (2010).
[8]F. Fukuyo, S. Ochiai, H. Miyake, K. Hiramatsu, H. Yoshida, and Y. Kobayashi, Jpn. J. Appl. Phys., Part 1 **52**, 01AF03 (2013).
[9]P. Cantu, F. Wu, P. Waltereit, S. Keller, A. E. Romanov, U. K. Mishra, S. P. DenBaars, and J. S. Speck, Appl. Phys. Lett. **83**, 674 (2003).
[10]S. Kurai, K. Shimomura, H. Murotani, Y. Yamada, H. Miyake, and K. Hiramatsu, J. Appl. Phys. **112**, 033512 (2012).
[11]S. Kurai, F. Ushijima, Y. Yamada, H. Miyake, and K. Hiramatsu, Jpn. J. Appl. Phys., Part 1 **52**, 08JL07 (2013).
[12]S. Tanaka, M. Takeuchi, and Y. Aoyagi, Jpn. J. Appl. Phys., Part 2 **39**, L831 (2000).
[13]O. Klein, J. Biskupek, K. Forghani, F. Scholz, and U. Kaiser, J. Cryst. Growth **324**, 63 (2011).
[14]Y. Taniyasu, M. Kasu, and N. Kobayashi, Appl. Phys. Lett. **81**, 1255 (2002).
[15]Y. Shimahara, H. Miyake, K. Hiramatsu, F. Fukuyo, T. Okada, H. Takaoka, and H. Yoshida, Appl. Phys. Express **4**, 042103 (2011).
[16]A. Uedono, K. Tenjinbayashi, T. Tsutsui, Y. Shimahara, H. Miyake, K. Hiramatsu, N. Oshima, R. Suzuki, and S. Ishibashi, J. Appl. Phys. **111**, 013512 (2012).
[17]H. Murotani, Y. Yamada, H. Miyake, and K. Hiramatsu, Appl. Phys. Lett. **98**, 021910 (2011).
[18]H. Murotani, D. Akase, K. Anai, Y. Yamada, H. Miyake, and K. Hiramatsu, Appl. Phys. Lett. **101**, 042110 (2012).
[19]S. Watanabe, N. Yamada, M. Nagashima, Y. Ueki, C. Sasaki, Y. Yamada, T. Taguchi, K. Tadatomo, H. Okagawa, and H. Kudo, Appl. Phys. Lett. **83**, 4906 (2003).
[20]S. Kurai, F. Ushijima, H. Miyake, K. Hiramatsu, and Y. Yamada, J. Appl. Phys. **115**, 053509 (2014).

Reuse of AIP Publishing content is subject to the terms at: https://publishing.aip.org/authors/rights-and-permissions. Download to IP: 133.62.137.102 On: Wed, 16 Mar 2016 07:53:26